Available online at www.sciencedirect.com
SCIENCE DIRECT®
Ultrasonics 43 (2005) 173–181
Ultrasonics
www.elsevier.com/locate/ultras

Finite element modelling of dense and porous piezoceramic disc hydrophones

R. Ramesh *, H. Kara, C.R. Bowen

Materials Research Centre, Department of Engineering and Applied Sciences, University of Bath, Bath BA2 7AY, UK

Received 10 February 2004; received in revised form 30 April 2004; accepted 1 May 2004
Available online 7 June 2004

Abstract

The acoustic characteristics of dense and porous piezoceramic disc hydrophones have been studied by finite element modelling (FEM). The FEM results are validated initially by an analytical model for a simple disc of dense piezoceramic material and then it is extended to a porous piezoceramic disc replicating a foam-reticulated sample. Axisymmetric model was used for dense piezoceramic hydrophone due its regular geometric shape. 3-dimensional model was used for the porous piezoceramics, since the *unit cell* model is inadequate to fully represent transducers of finite lateral dimensions. The porous PZT discs have been synthesised by foam-reticulation technique. The electrical impedance and the receiving sensitivity of the hydrophones in water are evaluated in the frequency range 10–100 kHz. The model results are compared with the experimental data. The receiving sensitivity of piezocomposite hydrophones is found to be reasonably constant over the frequency range studied. The sharp resonance peaks observed for the dense piezoceramic hydrophone has broadened to a large extent for porous piezoceramic hydrophones, indicating higher losses. The flat frequency response suggests that the 3–3 piezocomposites are useful for wide-band hydrophone applications.

PACS: 43.38.Fx
Keywords: Piezoceramics; Piezocomposites; Porous structures; Modelling; Hydrophones; Underwater acoustics

1. Introduction

Piezocomposite materials have drawn considerable attention in recent years due to their application in ultrasonic and underwater transducers [1,2]. Piezocomposites have higher electromechanical coupling coefficient, lower acoustic impedance and higher hydrostatic coefficients compared to the conventional Lead Zirconate Titanate (PZT) materials. Further, by changing the ceramic/polymer volume fractions, the material parameters of a composite transducer can be altered to meet specific requirements [3]. Although piezocomposite of various connectivities do exist [4], only composites with 1–3, 2–2 and 3–3 connectivities have been found to be more useful for transducer applications [5–7].

1–3 piezocomposites have been studied extensively and various modelling and experimental studies have been reported in literature [8,9]. Although, 1–3 composites are highly useful for transducer applications, their production is tedious and expensive [5]. 3–3 piezocomposites prove to be an alternative, with comparable material properties and relatively simpler method of synthesis [10]. 3–3 piezocomposites in the form of porous PZT materials show considerably improved transducer characteristics. Experimental studies on porous piezoelectric structures indicate that they have high hydrostatic figure-of-merit [10] and high receiving sensitivity [11,12]. However, their depth-handling capability and the stability to hydrostatic pressure have yet to be proved. The mechanical strength of the transducer can be improved by filling with a polymer as second phase.

In certain cases, depending on the method of synthesis, the 3–3 piezocomposites are found to coexist with 0–3 composites for intermediate ceramic volume fractions. The material properties of these composites with mixed connectivities can be evaluated using theoretical models [13,14]. Some theoretical models have been

* Corresponding author. NPOL, Thrikkakara, Cochin 682 021, India.
E-mail address: ramesh_rmani@hotmail.com (R. Ramesh).

0041-624X/$ - see front matter © 2004 Elsevier B.V. All rights reserved.
doi:10.1016/j.ultras.2004.05.001

proposed to study the material properties of ideal 3–3 piezocomposites [15–17]. However, the transducer characteristics of these materials have not been studied extensively, for which finite element modelling (FEM) would be a simple and effective tool. FEM studies on 1–3 piezocomposite transducers have been reported [18]. In these studies, only one *unit cell* of the composite block has been modelled, assuming that it represents the entire piezocomposite structure. Although these models can give material parameters like piezoelectric coefficients, to considerable accuracy, they are inadequate to predict the lateral-mode resonance of a transducer of finite dimensions. Hence, real-size 3-dimensional FEM studies are necessary to evaluate the device characteristics of piezocomposite hydrophones.

We have developed axisymmetric and 3-dimensional finite element models for dense PZT and porous PZT hydrophones, respectively. The axisymmetric FEM model is validated by a simple 3-dimensional analytical model. The model results of dense and porous piezoceramic hydrophones are compared with the experimental data and presented in this paper.

2. Finite element model

The hydrophones are modelled by using the finite element modelling package, ANSYS. We have followed two different approaches for modelling the hydrophones with dense PZT and porous PZT discs as active elements. Because of the regular geometric shape of dense PZT disc, a 2-dimensional axisymmetric model is sufficient. However, a real-size 3-dimensional model is needed for the porous PZT disc of finite size. The free-field voltage sensitivity and the electrical impedance of the hydrophones are of interest.

2.1. Hydrophones with dense PZT discs

Due to the simplicity in geometry, the dense PZT disc hydrophones are modelled by using 2-dimensional axisymmetric harmonic analysis. Consider a PZT solid cylinder (disc) of length L and radius a as shown in Fig. 1. Uniform electrodes are coated on the top and bottom flat surfaces and it is poled in the axial direction. The hydrophone is encapsulated by an acoustically transparent rubber and is surrounded by water medium.

The details of the axisymmetric model and the finite element mesh are shown in Fig. 2. Axisymmetric coupled-field elements are used for the active material. The model includes the PZT hydrophone and the surrounding fluid (water) medium. A small section of the fluid medium, which is in contact with the solid elements is assigned with acoustic elements capable of handling fluid-structure interactions. In all other fluid elements, the displacement degree of freedom (d.o.f) has been

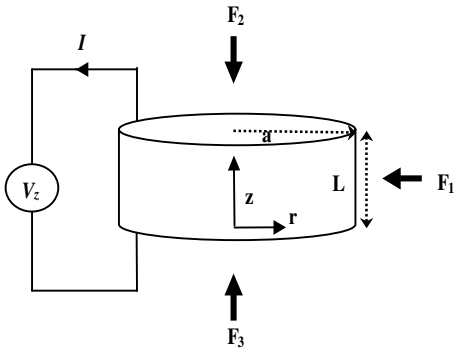

Fig. 1. Schematic diagram and the coordinates of an axially polarised piezoelectric disc transducer. Top and bottom surfaces are fully electroded. F_1, F_2 and F_3 are the forces acting on the surfaces.

suppressed. This significantly reduces the memory requirement and the computing time. The outer boundary of the fluid mesh contains infinite acoustic damping elements. This ensures that the acoustic waves are not reflected at the boundary, simulating the infinite extent of the fluid medium. In order to obtain better numerical accuracy, the size of the mesh has been kept small compared to the dominant wavelength of the sound waves in PZT as well as in water in the vicinity of the hydrophone. That means, the mesh size has been maintained to be less than or equal to $\lambda/5$ of the highest frequency (100 kHz) studied.

The nodes lying on the top and bottom electrode surfaces of the PZT disc are coupled individually and voltage d.o.f is activated. Nodes on all outer surfaces are coupled and pressure d.o.f is activated. Two different boundary conditions are applied for the present studies. In the case of the receiving sensitivity measurement, an acoustic wave of known pressure P excites the transducer from the fluid medium and the voltage generated at the electrodes is determined. For electrical impedance measurement, the outer surfaces of the transducer are stress-free and a known voltage is applied between the electrodes. Impedance is calculated from the charge collected at the electrodes. Harmonic analysis with no damping is performed in the frequency range 10–100 kHz.

2.2. Hydrophones with porous PZT discs

The porous PZT has an intricate structure that cannot be analysed using a 2-dimensional model. Hence, we have used a 3-dimensional model to characterise hydrophones with porous structures of 3–3 piezocomposites with finite dimensions.

In modelling piezocomposites, it has been a general practice to model only an *unit cell* of the structure, assuming that it is representative of the entire piezocomposite structure [18]. However in certain cases, the results of the *unit cell* model deviate from the actual values, especially in the determination of resonance

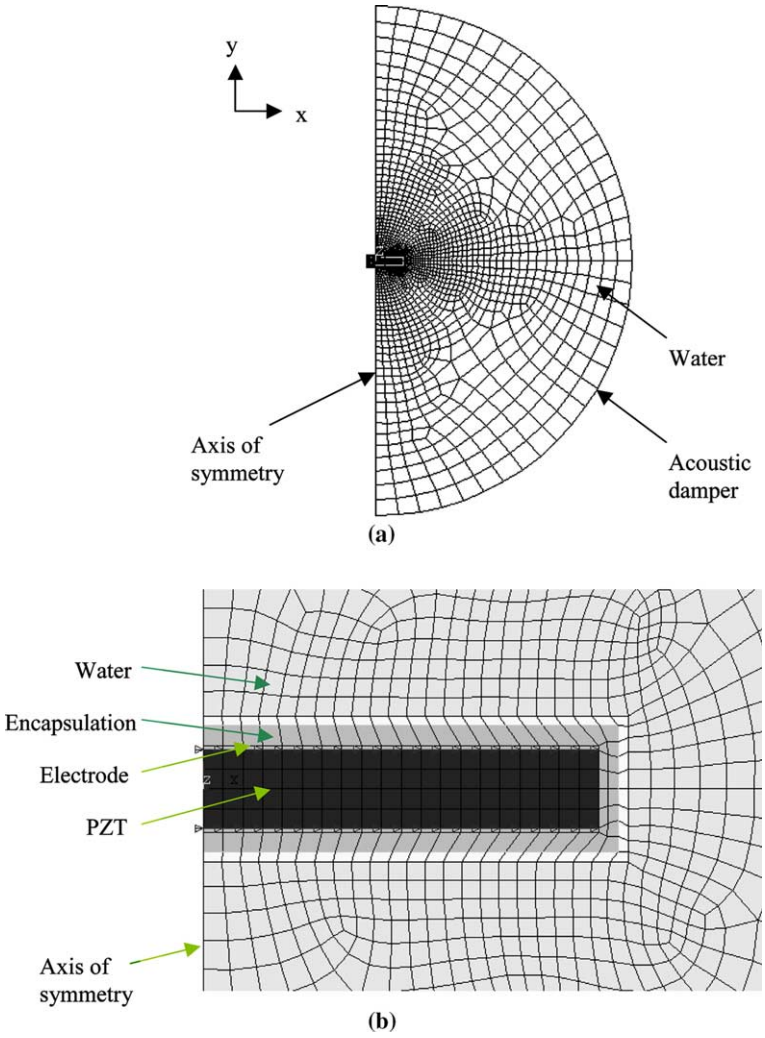

Fig. 2. (a) The axisymmetric finite element model of a dense PZT hydrophone and (b) the enlarged view of the model.

frequencies [19]. The *unit cell* model can correctly predict the resonance frequencies corresponding to the thickness-mode vibrations, whereas it cannot predict the lateral-mode (radial-mode) resonance frequencies if the lateral dimensions of the transducers are finite and comparable to the thickness. Even, the application of periodic boundary conditions can only simulate the infinite extent of the lateral dimensions (x–y plane). Further, in the case of transducers with finite dimensions, the resonance frequency corresponding to the dimension in the z-direction depends also on the dimensions in the x- and y- directions [19]. It is therefore necessary to use a real-dimensional model. Hence, we have performed finite element analysis of a real-size 3-dimensional model of the porous PZT hydrophone, despite the requirement of large computer memory size and a prolonged computing time involved.

The porous piezoceramic structure used in the finite element model of a 3–3 piezocomposite hydrophone is shown in Fig. 3. This is chosen to be as close to the practical structure of a foam-reticulated sample described in the following section. The complete 3-D model along with the surrounding fluid medium is shown in Fig. 4. One fourth of the geometry is modelled due to symmetry and the plane of symmetry boundary

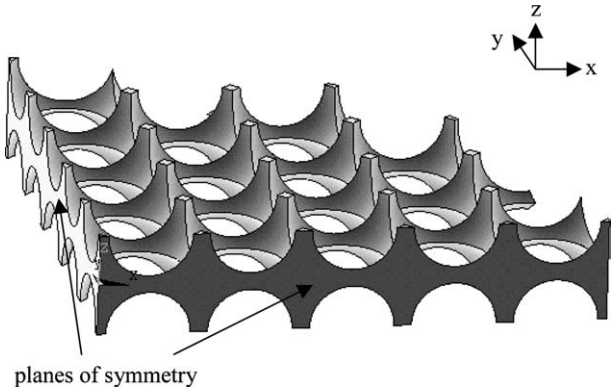

Fig. 3. Structure of a porous PZT disc. 1/4th of the model is shown.

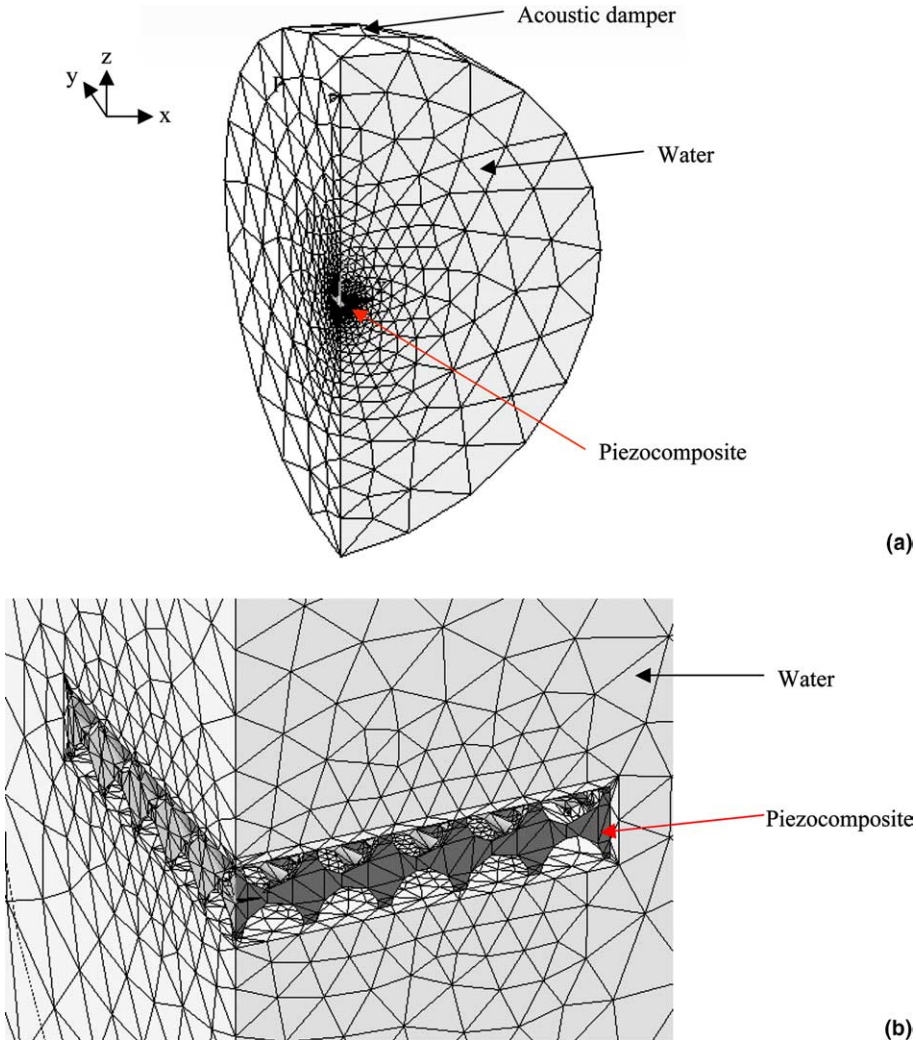

Fig. 4. (a) The 3-dimensional finite element model of a porous PZT hydrophone and (b) the enlarged view of the model.

conditions are applied on the *xz* and *yz* planes. Although 1/8th model could save considerable computing time, the non-symmetry of the electric potential along the *z*-axis does not allow such possibility in the present model.

The ceramic volume fraction of the piezocomposite disc is taken as 22%. The receiving sensitivity and electrical impedance are evaluated in two successive analyses imposing appropriate boundary conditions. The boundary conditions are same as those of the dense PZT hydrophone explained previously.

3. Experimental

Dense PZT discs were made by compacting the PZT5H powder and sintering at 1200 °C for 2 h. Porous PZT structures were made by replicating polyethylene foams with PZT slip, followed by polymer removal and sintering [10]. These structures can be considered as 3–3 piezocomposites with no second phase of polymers. The

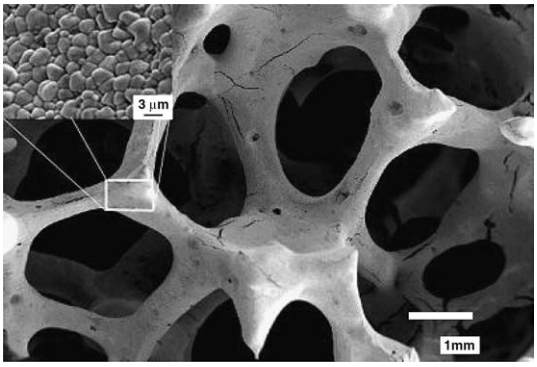

Fig. 5. SEM picture of a porous PZT material synthesised by foam-reticulation technique.

scanning electron micrograph (SEM) of the foam-reticulated sample is shown in Fig. 5. The ceramic volume fraction of the porous structure is found to be 22%. The thickness and diameter of the discs are 4 and 40 mm, respectively. The piezoelectric discs were characterised

by measuring piezoelectric charge coefficient (d_{33}) and dielectric permittivity (ε_r). The top and bottom surfaces were fully electroded by applying air-drying silver paint and the discs were polarised in air along the axial direction at an electric field of 2 kV/mm at 110 °C. Hydrophones were assembled and encapsulated with polyurethane rubber to make it water-worthy. The free-field voltage sensitivity was measured in a water tank using impulse technique [20] in the frequency range 10–100 kHz and electrical impedance was measured using Solartron Impedance Analyser (model 1260).

4. Results and discussion

Two types of hydrophones, one with dense PZT disc and another with porous PZT disc are considered for the present analysis. Both types of hydrophones are studied by FEM and only the first type was studied by a simple 3D analytical model presented in Appendix A. The material parameters used for the analytical and the finite element modelling are given in Table 1. Same boundary conditions are imposed for the analytical and the finite element models, i.e. the pressure of the incident sound waves is 1 Pa for receiving sensitivity calculation and the potential difference between the electrodes is 1 V for impedance calculations.

Table 1
Material parameters used in the model calculations. Data for PZT5H are taken from Ref. [25] and typical values are taken for other materials

Parameter	Value
I. PZT5H	
(a) Elastic coefficients (10^{10} Nm^{-2})	
c_{11}^D	13.03
c_{12}^D	8.33
c_{13}^D	7.33
c_{33}^D	15.89
c_{44}^D	4.22
c_{66}^D	2.4
(b) Piezoelectric coefficients (10^9 Vm^{-1})	
h_{31}	−0.5
h_{33}	1.8
h_{15}	1.13
(c) Density (kg m^{-3})	7500
(d) Dielectric constant	1470
II. Electrode	
(a) Density (kg m^{-3})	8250
(b) Young's modulus (GPa)	110
(c) Poisson's ratio	3.4
III. Encapsulation	
(a) Density (kg m^{-3})	940
(b) Young's modulus (MPa)	2.0
(c) Poisson's ratio	0.45
IV. Water	
(a) Density (kg m^{-3})	1000
(b) Velocity of sound (m s^{-1})	1460

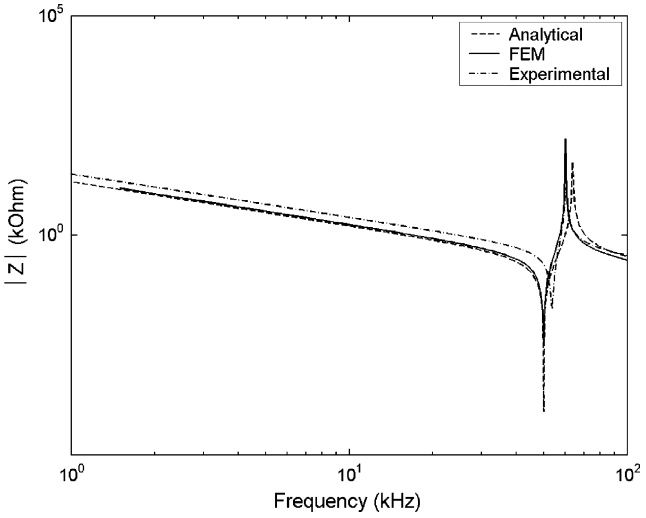

Fig. 6. Electrical impedance spectrum of dense PZT hydrophone.

The electrical impedance spectrum for the dense piezoceramic hydrophone in the frequency range 10–100 kHz obtained by analytical, FEM and experimental studies are shown in Fig. 6. The resonance peaks observed at around 50 kHz correspond to the fundamental radial-mode of vibrations. The analytical model considers only the normal stresses acting on the surfaces. The continuity of stress at the boundaries is satisfied in an average sense. With these approximations, the present model could predict the fundamental mode of resonance. A similar behaviour has been reported for piezoceramic solid cylinders of arbitrary aspect ratio [21]. However, only an exact model [22] can precisely predict all the higher harmonics.

The impedance data for the porous piezoceramic hydrophone obtained by FEM and experimental studies are shown in Fig. 7. In this case, the resonance peaks have almost disappeared, indicating the weak coupling.

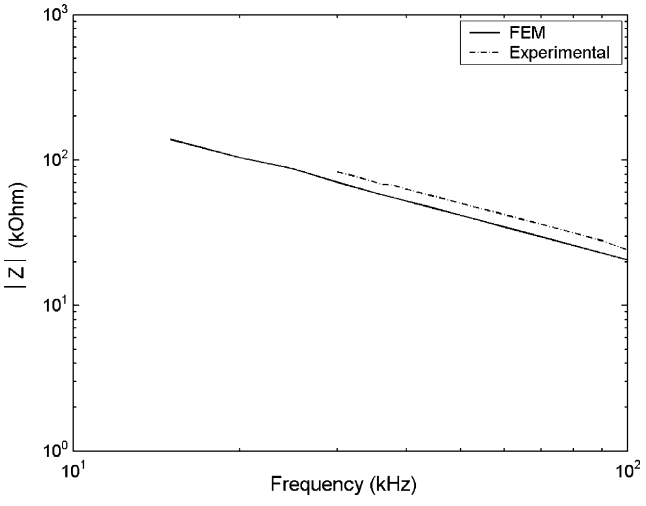

Fig. 7. Electrical impedance spectrum of porous PZT hydrophone.

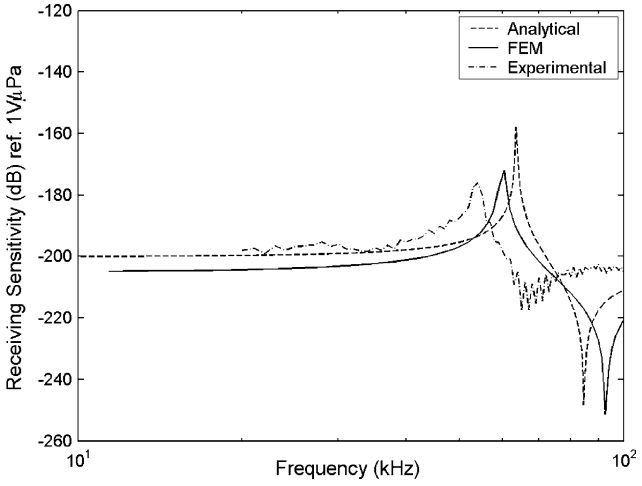

Fig. 8. Receiving sensitivity of dense PZT hydrophone as a function of frequency.

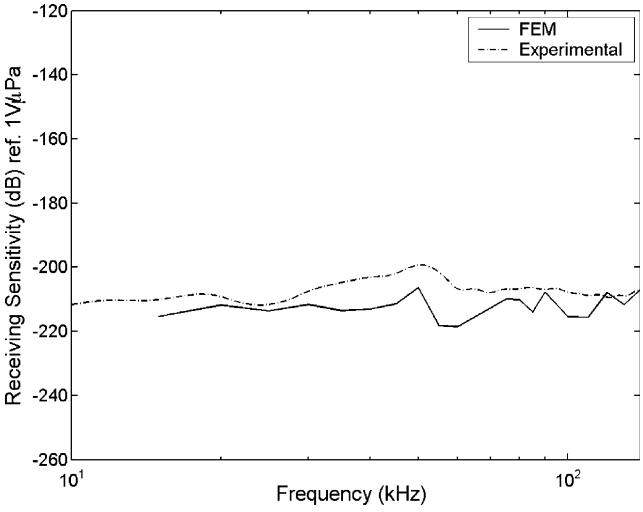

Fig. 9. Receiving sensitivity of porous PZT hydrophone as a function of frequency.

Fig. 8 shows the free-field voltage sensitivity in water for the dense PZT hydrophone obtained by analytical model, finite element model and experimental studies. In the analytical model, the effect of encapsulation and water loading are not considered. This could lead to a shift in the resonance frequencies as seen in the figure. The polyurethane rubber used for encapsulating the hydrophone has acoustic impedance close to that of water and hence is assumed to be acoustically transparent. It can be seen from the figure that the sensitivity curve is flat for frequencies below 50 kHz. The radial mode resonance appearing at around 50 kHz is not generally desirable for hydrophone applications, since it limits the operating range of frequency. An ideal hydrophone has a constant receiving sensitivity over a wide frequency range [23]. The resonance peaks can be shifted beyond the operating range by carefully selecting the dimensions of the active elements.

Fig. 9 shows the receiving sensitivity of the piezocomposite hydrophones obtained by FEM and experimental studies. The sensitivity value is found to be around −210 dB (re. 1 V/μ Pa) and is fairly constant in the frequency range studied. These values are comparable to the experimental values of −(200–205) dB reported for single-element hydrophones with 75% porosity at 100 kHz [12]. A 3×3 array of porous piezoceramic hydrophone, however, shows a higher sensitivity of −193 dB below resonance [7].

FEM studies were limited to 10 kHz in the low frequency side in order to compare with the experimental results, which could not be collected for frequencies below 10 kHz due to limitations in the experimental set up. Ideal porous structures are considered for the finite element model. However, the scanning electron micrographs show the presence of some amount of micro-cracks in the experimentally synthesised foam-reticulated samples. This could lead a small difference between the experimental and model results as seen in Fig. 9.

It can be seen from the figures that the resonance peaks corresponding to the radial-mode vibrations are very prominent for dense PZT hydrophone and have weakened to a large extent for piezocomposites. This may be due to higher dielectric and mechanical losses of the composites compared to those of dense piezoceramic materials. The sensitivity response is found to be reasonably flat over a wide frequency range. This is particularly advantageous as these hydrophones can be used for wide-band applications.

5. Conclusions

Axisymmetric and 3-dimensional finite element models have been developed to characterise dense piezoceramic and 3–3 piezocomposite hydrophones, respectively. Since the *unit cell* model is inadequate to fully evaluate transducers of finite dimensions, a real-size finite element model has been developed for 3–3 piezocomposites. The electrical impedance and the receiving sensitivity of the hydrophones in water evaluated by the analytical model and the finite element model agree reasonably well with the experimental results. This indicates that the finite element modelling can be used to design a 3–3 piezocomposite transducer with desired performance, by altering the design variables such as ceramic volume fraction, dimensions and orientations of the pores. The broadening of resonance peaks of porous piezoceramic hydrophones results in a flat frequency response. This suggests that the 3–3 piezocomposites can be used for wide-band hydrophone applications.

Acknowledgements

The authors wish to thank Dr. N. Jayasundare and Dr. V. Humphrey, Department of Physics, University of Bath, for their help in experimental measurements of receiving sensitivity. One of the authors (RR) is grateful to the Department of Science and Technology, New Delhi, India for providing financial assistance and the Director, NPOL for permission to undertake this research work.

Appendix A. Analytical model

An axisymmetric analytical model is presented for a dense piezoelectric disc of arbitrary aspect ratio. Consider a piezoceramic disc of radius a and thickness L, as shown in Fig. 1. The top and bottom surfaces are fully electroded and the piezoceramic disc is polarised in the axial direction. Cylindrical coordinate system (r, θ, z) is considered. The excitation and response of the disc are considered to be axisymmetric and hence all the parameters are independent of θ. The electrical impedance and the open-circuit voltage sensitivity are of interest.

The piezoelectric constitutive equations are written as [24],

$$T_{rr} = c_{11}^D S_{rr} + c_{12}^D S_{\theta\theta} + c_{13}^D S_{zz} - h_{31} D_z \tag{A.1a}$$

$$T_{\theta\theta} = c_{12}^D S_{rr} + c_{11}^D S_{\theta\theta} + c_{13}^D S_{zz} - h_{31} D_z \tag{A.1b}$$

$$T_{zz} = c_{13}^D (S_{rr} + S_{\theta\theta}) + c_{33}^D S_{zz} - h_{33} D_z \tag{A.1c}$$

$$E_z = -h_{31}(S_{rr} + S_{\theta\theta}) - h_{33} S_{zz} + \beta_{33}^S D_z \tag{A.1d}$$

where T's are the components of stress, S's are the components of strain, h's are the piezoelectric coefficients, β_{33}^S is the dielectric impermittivity, D_z is the charge density, c^D's are the elastic stiffness coefficients at constant D and E_z is the electric field given by,

$$E_z = -\frac{\partial \varphi}{\partial z} \tag{A.2}$$

where φ is the electric potential. The components of strain are written as,

$$[S_{rr}, \quad S_{\theta\theta}, \quad S_{zz}] = \left[\tfrac{\partial W}{\partial r}, \quad \tfrac{W}{r}, \quad \tfrac{\partial U}{\partial z}\right] \tag{A.3}$$

where W and U are the displacements in the radial and axial directions, respectively.

Using the non-vanishing components of the elastic, piezoelectric and dielectric matrices of a transversely isotropic piezoelectric material belonging to the crystal class ∞mm, the equilibrium equations are written as,

$$\frac{\partial T_{zz}}{\partial z} = -\rho\omega^2 U \tag{A.4a}$$

$$\frac{\partial T_{rr}}{\partial r} + \frac{1}{r}(T_{rr} - T_{\theta\theta}) = -\rho\omega^2 W \tag{A.4b}$$

where ρ is the density and ω is the angular frequency. The term $e^{j\omega t}$ has been suppressed in all equations for convenience. The components of shear stress are assumed to be zero.

The axisymmetric equations of motion can be written in terms of the components of displacements by substituting Eqs. (A.1) and (A.3) in Eq. (A.4) as follows,

$$c_{33}^D \frac{\partial^2 U}{\partial z^2} = -\rho\omega^2 U \tag{A.5a}$$

and

$$c_{11}^D \left[\frac{\partial^2 W}{\partial r^2} + \frac{1}{r}\frac{\partial W}{\partial r} - \frac{W}{r^2}\right] = -\rho\omega^2 W \tag{A.5b}$$

Solutions to these equations can be written in the form,

$$U = A\sin(k_z z) + B\cos(k_z z) \tag{A.6a}$$

and

$$W = CJ_1(k_r r) \tag{A.6b}$$

where A, B and C are the constants to be determined using a given boundary conditions, k_z and k_r are the wave numbers in the axial and radial directions, respectively as given by,

$$k_z = \omega\sqrt{\frac{\rho}{c_{33}^D}} \quad \text{and} \quad k_r = \omega\sqrt{\frac{\rho}{c_{11}^D}} \tag{A.7}$$

and J_1 is the first order Bessel function of the first kind. In order to satisfy the finiteness condition at the origin of the disc ($r = 0$), the Bessel function of the second kind $Y_1(k_r, r)$ has been excluded in the solution (A.6b). It has to be included for a hollow cylinder.

From these equations, the other parameters of interest, such as the stress acting on the surfaces and the charge developed on the electrodes can be easily determined. The radial and axial components of the normal stress can be obtained by substituting Eqs. (A.3) and (A.6) in (A.1) as given by,

$$T_{rr} = Ac_{13}^D k_z \cos(k_z z) - Bc_{13}^D k_z \sin(k_z z) + C\left[c_{11}^D k_r J_0(k_r r) + \left(c_{12}^D - c_{11}^D\right)\frac{1}{r}J_1(k_r r)\right] - h_{31} D_z \tag{A.8}$$

and

$$T_{zz} = Ac_{33}^D k_z \cos(k_z z) - Bc_{33}^D k_z \sin(k_z z) + Cc_{13}^D k_r J_0(k_r r) - h_{33} D_z \tag{A.9}$$

Similarly, the charge density can be written as,

$$E_z = -Ah_{33} k_z \cos(k_z z) + Bh_{33} k_z \sin(k_z z) - Ch_{31} k_r J_0(k_r r) + \beta_{33}^S D_z \tag{A.10}$$

where $D_z = I_z / j\omega\pi a^2$.

In order to evaluate the transducer characteristics, it is convenient to use force instead of stress. The radial and axial components of force are obtained by integrating Eq. (A.8) over the curved surface at $r = a$ and Eq. (A.9) over the flat surface at $z = L$, respectively. Therefore we get,

$$\begin{aligned} F_{rr} &= 2\pi a \int_0^L T_{rr}\,\mathrm{d}z \\ &= Ac_{13}^D k_z 2\pi a \sin(k_z L) + Bc_{13}^D k_z 2\pi a[\cos(k_z L) - 1] \\ &\quad + C2\pi aL\left[c_{11}^D k_r J_0(k_r a) + \left(c_{12}^D - c_{11}^D\right)\frac{1}{r}J_1(k_r a)\right] \\ &\quad - \frac{I_z h_{31} 2L}{j\omega a} \end{aligned} \tag{A.11}$$

$$\begin{aligned} F_{zz} &= 2\pi \int_0^a T_{zz} r\,\mathrm{d}r \\ &= Ac_{33}^D k_z \pi a^2 \cos(k_z L) - Bc_{33}^D k_z \pi a^2 \sin(k_z L) \\ &\quad + Cc_{13}^D 2\pi a J_1(k_r a) - \frac{I_z h_{33}}{j\omega} \end{aligned} \tag{A.12}$$

The voltage is obtained by integrating E_z in Eq. (A.10) with respect to r over the electrode surface and using the relation, $V = -\int_0^L E_z\,\mathrm{d}z$ as given by,

$$\begin{aligned} V &= Ah_{33}\sin(k_z L) + Bh_{33}[\cos(k_z L) - 1] \\ &\quad - Ch_{31}J_1(k_r a)2L/a - \frac{I_z \beta_{33}^S L}{j\omega\pi a^2} \end{aligned} \tag{A.13}$$

A.1. Receiving sensitivity

The hydrophone is excited by a pressure wave propagating from the +ve z-direction. The potential difference developed across the electrodes is of interest. The mechanical and electrical boundary conditions are (i) the continuity of forces on the outer surfaces and (ii) the open-circuit, respectively as given by,

$$F_{rr} = F_1 \quad \text{on } 0 \leqslant z \leqslant L \text{ at } r = a \tag{A.14a}$$

$$F_{zz} = F_2 \quad \text{on } 0 \leqslant r \leqslant a \text{ at } z = L \tag{A.14b}$$

$$F_{zz} = F_3 \quad \text{on } 0 \leqslant r \leqslant a \text{ at } z = 0 \tag{A.14c}$$

and

$$I_z = 0 \quad \text{on } 0 \leqslant r \leqslant a \text{ at } z = L \tag{A.14d}$$

where F_1, F_2 and F_3 are the forces acting on the curved surface, top surface and bottom surface, respectively as shown in Fig. 1. By applying these boundary conditions in Eqs. (A.11)–(A.13), we get four simultaneous equation with four unknowns A, B, C and I_z as written in a matrix form,

$$[M]\begin{Bmatrix} A \\ B \\ C \\ V \end{Bmatrix} = \begin{Bmatrix} F_1 \\ F_2 \\ F_3 \\ 0 \end{Bmatrix} \tag{A.15}$$

where $[M]$ is the 4×4 coefficient matrix. The receiving voltage sensitivity can be obtained by using the relation,

$$FFVS = \frac{V}{F} \tag{A.16}$$

A.2. Electrical impedance

The electrical impedance of the transducer can be determined by imposing a stress-free boundary condition on all the surfaces ($F = 0$) and a known voltage (V_0) across the electrodes.

By applying the boundary conditions in Eqs. (A.11)–(A.13) and re-arranging the equations, we get,

$$[N]\begin{Bmatrix} A \\ B \\ C \\ I_z \end{Bmatrix} = \begin{Bmatrix} 0 \\ 0 \\ 0 \\ V_0 \end{Bmatrix} \tag{A.17}$$

where $[N]$ is the 4×4 coefficient matrix. The electrical impedance can be obtained by using the relation,

$$Z = \frac{V_0}{I_z} \tag{A.18}$$

References

[1] D.P. Skinner, R.E. Newnham, L.E. Cross, Flexible composite transducers, Mater. Res. Bull. 13 (1978) 599–607.

[2] W.A Smith, The role of piezocomposites in ultrasonic transducers, IEEE Ultrason. Symp. Proc. (1989) 755–766.

[3] W.A. Smith, Tailoring the composite piezoelectric materials for medical ultrasonic transducers, Proc. IEEE Ultrason. Symp. Proc. (1985) 642–647.

[4] R.E. Newnham, D.P. Skinner, L.E. Cross, Connectivity and piezoelectric–pyroelectric composites, Mat. Res. Bull 13 (1978) 525–536.

[5] L. Bowen, R. Gentilman, D. Fiore, H. Pham, W. Serwatka, C. Near, B. Pazol, Design, fabrication and properties of sonopanel 1–3 piezocomposite transducers, Ferroelectrics 187 (1996) 109–120.

[6] Q.M. Zhang, J. Chen, H. Wang, J. Zhao, L.E. Cross, M.C. Trottier, A new transverse piezoelectric mode 2–2 piezocomposite for underwater transducer applications, IEEE Trans. Ultrason. Ferroelec. Freq. Control 42 (1995) 774–781.

[7] S. Marselli, V. Pavia, C. Galassi, E. Roncari, F. Cracium, G. Guidarelli, Porous piezoelectric ceramic hydrophone, J. Acous. Soc. Am. 106 (1999) 733–738.

[8] W.A. Smith, B.A. Auld, Modelling 1–3 composite piezoelectrics: thickness mode oscillations, IEEE Trans. Ultrason. Ferroelec. Freq. Control 38 (1991) 40–47.

[9] R. Ramesh, R.M.R. Vishnubhatla, Estimation of material parameters of lossy 1–3 piezocomposite plates by non-linear regression analysis, J. Sound Vib. 226 (1999) 573–584.

[10] H. Kara, R. Ramesh, R. Stevens, C.R. Bowen, Porous PZT ceramics for receiving transducers, IEEE Trans. Ultrason. Ferroelec. Freq. Control 50 (2003) 289.

[11] T. Arai, K. Ayusawa, H. Sato, T. Miyata, K. Kawamura, K. Kobayashi, Properties of hydrophones with porous piezoelectric ceramics, Jpn. J. Appl. Phys. 30 (1991) 2253–2255.

[12] K. Ina, T. Mano, S. Imura, K. Nagata, Hydrophone sensitivity of porous Pb(Zr,Ti)O_3 ceramics, Jpn. J. Appl. Phys. Part I 33 (1994) 5381–5384.
[13] T.E. Gomez, F. Montero deEspinosa, F. Levassort, M. Lethiecq, A. James, E. Ringgard, C.E. Millar, P. Hawkins, Ultrasonics 36 (1998) 907–923.
[14] F. Levassort, M. Lethiecq, R. Sesmare, L.P. Tran_huu_Hue, Effective electroelastic mosuli of 3–3 (3–0) piezocomposites, IEEE Trans. Ultason. Ferroelec. Freq. Control 46 (1999) 1028–1033.
[15] H. Banno, Effect of porosity on dielectric, elastic and electromechanical properties of Pb(Zr,Ti)O_3 ceramics with open pores: a theoretical approach, Jpn. J. Appl. Phys. Part I 32 (1993) 4214–4217.
[16] M.L. Dunn, M. Taya, Electromechanical properties of porous piezoelectric ceramics, J. Am. Ceram. Soc. 76 (1993) 1697–1706.
[17] C.R. Bowen, A. Parry, H. Kara, S.W. Mahon, Analytical modelling of 3–3 piezoelectric composites, J. Eur. Ceram. Soc. 21 (2001) 1463–1467.
[18] G. Hayward, J.A. Hossack, Finite element analysis of 1–3 composite piezoelectric transducers, IEEE Trans. Ultason. Ferroelec. Freq. Control 38 (1991) 618–629.
[19] W. Qi, W. Cao, Finite element analysis and experimental studies on the thickness resonance of piezocomposite transducers, Ultrason. Imaging 18 (1996) 1–9.
[20] R.J. Bobber, Underwater electroacoustic measurements, Naval Research Laboratory, Washington, USA, 1970.
[21] A. Iula, N. Lamberti, M. Pappalardo, An approximated 3-D model of cylinder shaped piezoceramic elements for transducer applications, IEEE Trans. Ultason. Ferroelec. Freq. Control 45 (1998) 1056–1064.
[22] D.D. Ebenezer, R. Ramesh, Exact analytical model of axially polarized piezoceramic cylinders with arbitrary boundary conditions on the flat surfaces, J. Acous. Soc. Am. Part 1 113 (4) (2003) 1900–1908.
[23] Bruel & Kjaer Application notes, Introduction to underwater acoustics, 1–34, Bruel & Kjaer, Denmark.
[24] IEEE standard on piezoelectricity, ANSI/IEEE Std 176-1987, The Institute of Electrical and Electronics Engineers, New York, USA.
[25] D. Berlincourt, H.H.A. Krueger, Important properties of Morgan Matroc Piezoelectric Ceramics, TP-226, Morgan Matroc Ltd., UK.